Electronic Supplementary Material (ESI) for ChemComm.
This journal is © The Royal Society of Chemistry 2021

Supporting information

An octacoordinated Nb atom in the $NbAl_8H_8^+$ cluster

Piero Ferrari,[a] Hung Tan Pham,[b] Jan Vanbuel,[a]
Minh Tho Nguyen,[c,*] André Fielicke[d] and Ewald Janssens[a,*]

[a] Quantum Solid-State Physics, KU Leuven, Celestijnenlaan 200D, 3001 Leuven, Belgium.
[b] Department of Chemistry, KU Leuven, Celestijnenlaan 200F, 3001 Leuven, Belgium.
[c] Institute for Computational Science and Technology (ICST) Ho Chi Minh City, Vietnam.
[d] Fritz-Haber-Institut der Max-Planck-Gesellschaft, Faradayweg 4−6, 14195 Berlin, Germany.

Email: ewald.janssens@kuleuven.be
Email: tho.nm@icst.org.vn

Content

1) Representative mass spectrum of $NbAl_nH_{2p}^+$ clusters

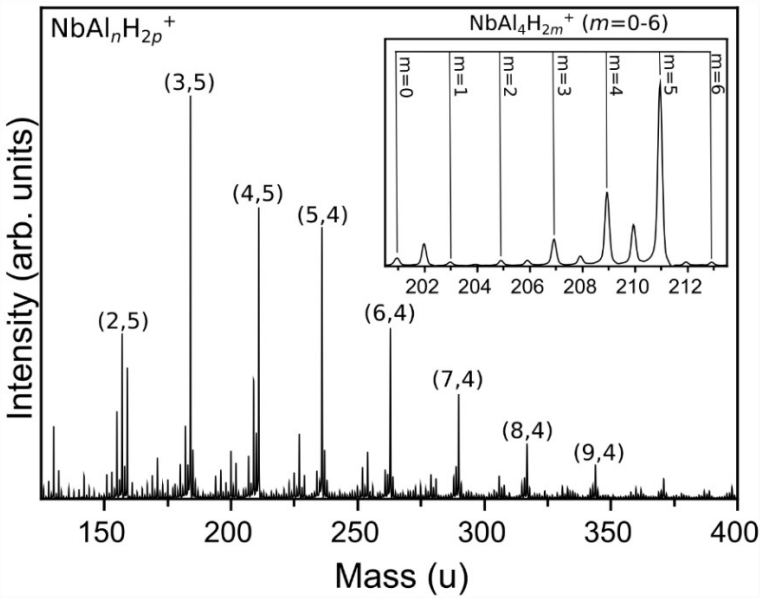

Figure S1. Representative mass spectrum of $NbAl_nH_{2p}^+$ clusters (n = 1 – 13, p = 0 – 6). The most intense peaks are labeled as (n,p). In between the peaks corresponding to the $NbAl_nH_{2p}^+$ series, clusters with two Nb atoms are present. The inset shows the abundances of $NbAl_4H_{2m}^+$ (m = 0 – 6). Additional peaks in between different m values correspond to complexes with an odd number of H atoms. These complexes are formed by a fraction of H_2 gas that dissociates in the plasma during cluster formation. Their contribution to the mass spectrum is estimated to be around 10 to 15%.

2) Infrared multiple photon dissociation spectra

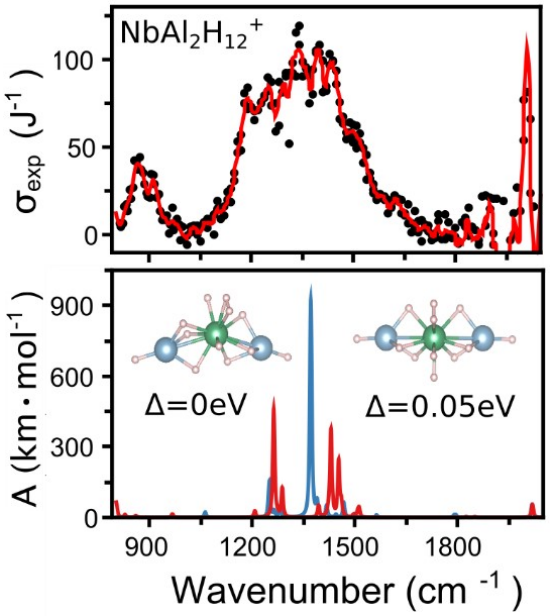

Figure S2. (top) IRMPD spectrum of $NbAl_2H_{12}^+$ (raw data in black, three-point moving average in red) and (bottom) calculated IR spectra of the lowest energy (blue, 0.0 eV) and second lowest energy (red, +0.05 eV) isomers of $NbAl_2H_{12}^+$.

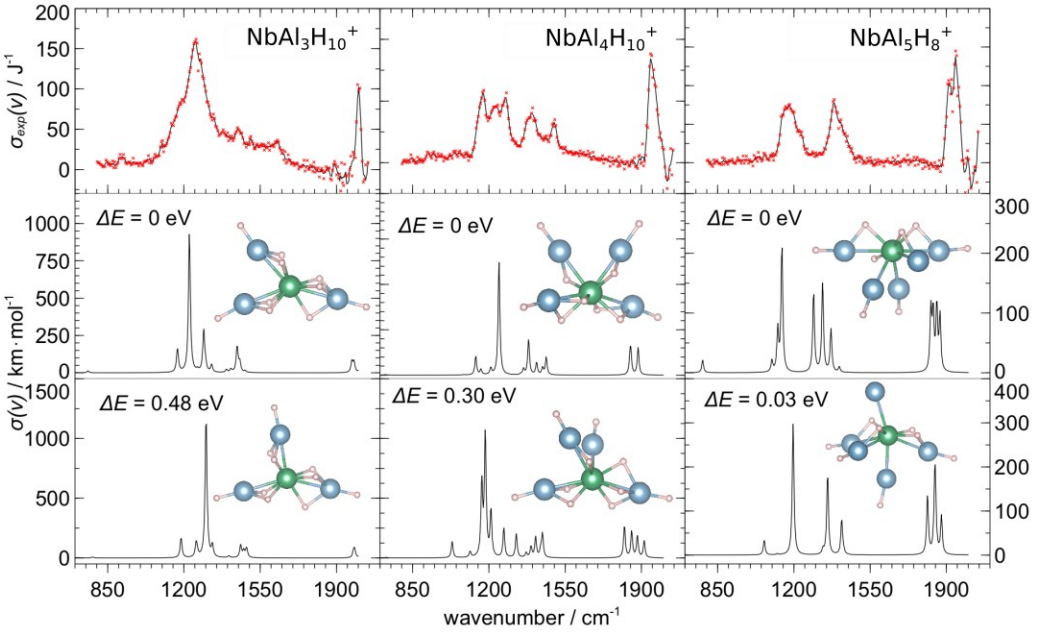

Figure S3. IRMPD spectra of $NbAl_3H_{10}^+$ (left) , $NbAl_4H_{10}^+$ (middle), and $NbAl_5H_8^+$ (right) and calculated IR spectra of the two lowest energy isomers for each of these clusters. The structures of the clusters are added as insets.

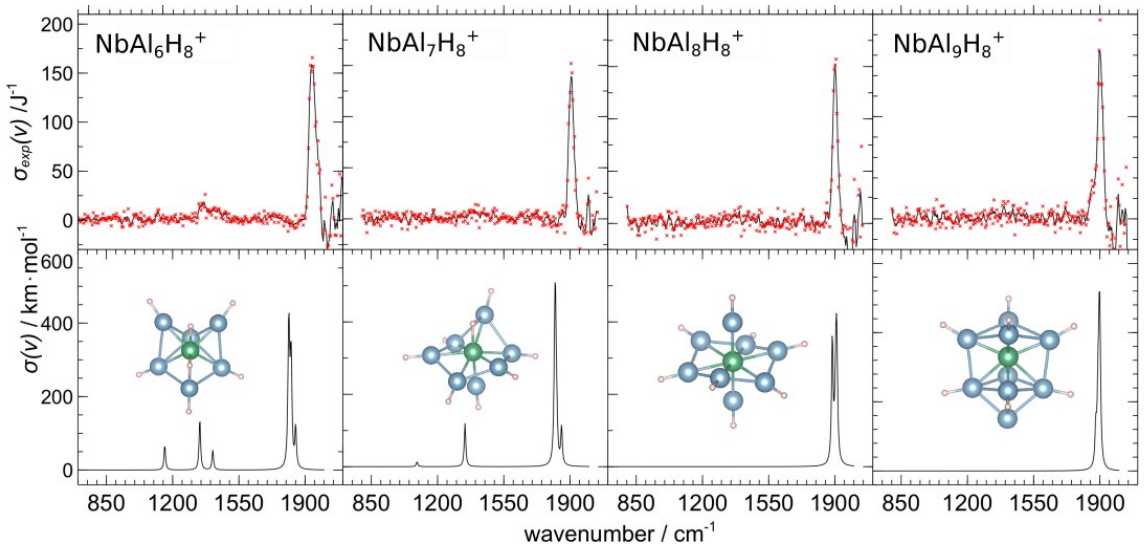

Figure S4. IRMPD spectra of $NbAl_nH_8^+$ (n = 6 – 9) and the calculated IR spectra of the lowest energy isomers for each of those clusters. The structures of the clusters are added as insets.

3) Benchmark analysis of theory level

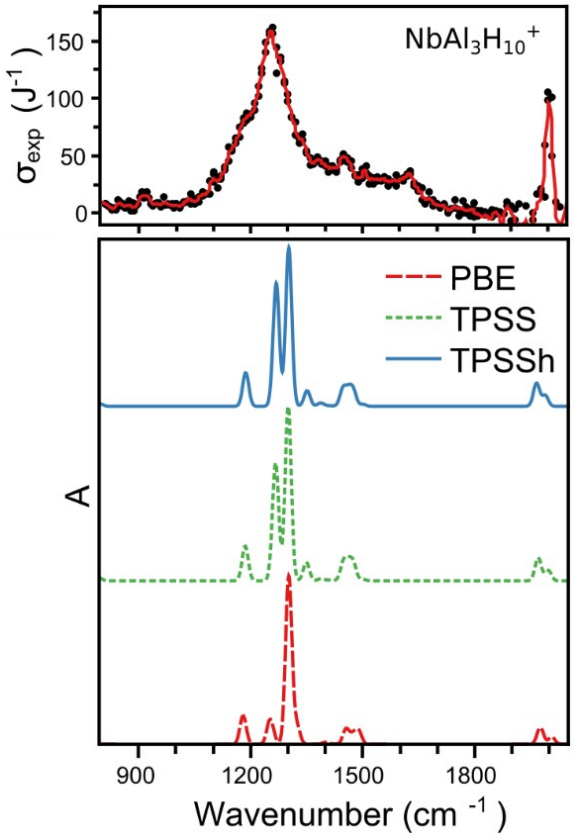

Figure S5. (top) IRMPD spectrum of $NbAl_3H_{10}^+$. (bottom) Calculated IR spectra using three functionals, PBE, TPSS and TPSSh. While the three functionals yield similar results, in fair agreement with the experimental data, TPSS and TPSSh reproduce better the broad feature observed at 1250 cm^{-1}, given the relative intensity of the bands calculated at 1270 and 1300 cm^{-1}.

4) Illustration of the vibrational modes involving hydrogen in $NbAl_8H_{2p}^+$ clusters

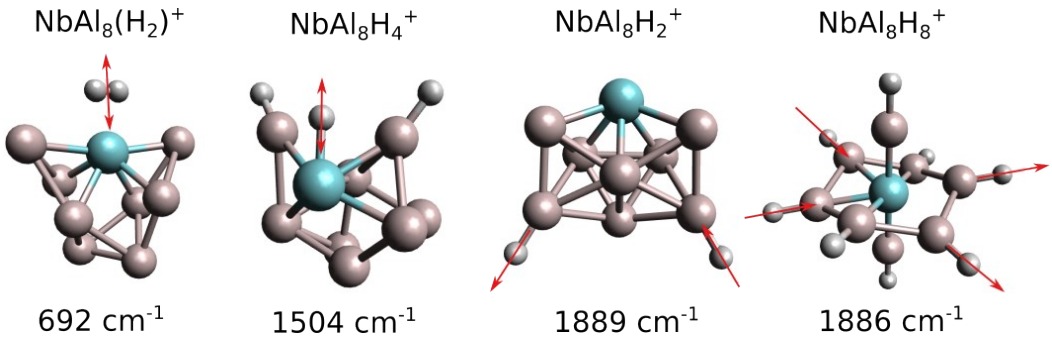

Figure S6. Representation of the displacement of atoms in selected vibrational modes of $NbAl_8H_{2p}^+$ clusters. Red arrows highlight the displacements of all H atoms; the displacements of the Al and Nb atoms are minor in these modes. Below each mode, the corresponding frequency is mentioned.

5) Electron density analysis of $NbAl_8H_8^+$

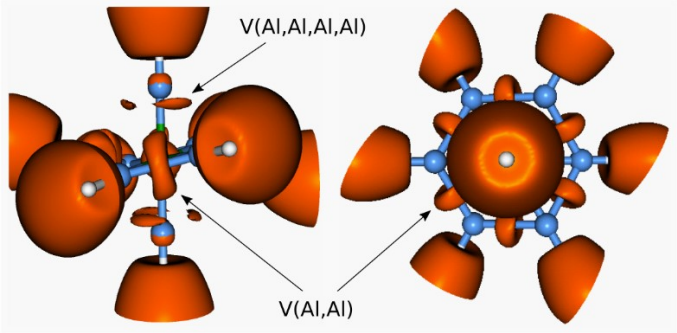

Figure S7. Plot of the electron localization function of $NbAl_8H_8^+$ (Iso1). A value ELF=0.8 is used. According to ELF, six AlH groups connect together through Al-Al bonds, forming a $(AlH)_6$ cycle, as indicated by the appearance of V(Al,Al) basins. There is no localization domain between the Nb atom and the $(AlH)_6$ cycle at the bifurcation value around 0.8. As a result, the electrostatic interaction has an important role in the bonding between Nb and the $(AlH)_6$ cycle. The top and bottom AlH groups form a delocalized bonding to the Nb@$(AlH)_6$ hexagonal cycle, as indicated by the appearance of three four synaptic (Al,Al,Al,Al) basins.

6) Orbital energy diagrams of $NbAl_8H_8^+$ and $NbAl_8H_6^+$

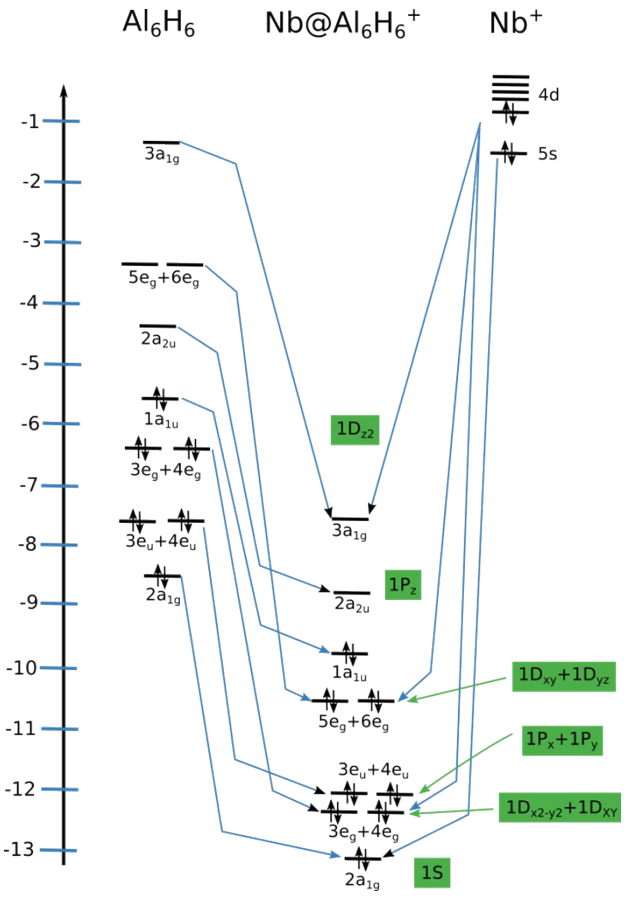

Figure S8. Orbital energy diagram illustrating the orbital interaction between Nb^+ and the Al_6H_6 cycle in Nb@$Al_6H_6^+$.

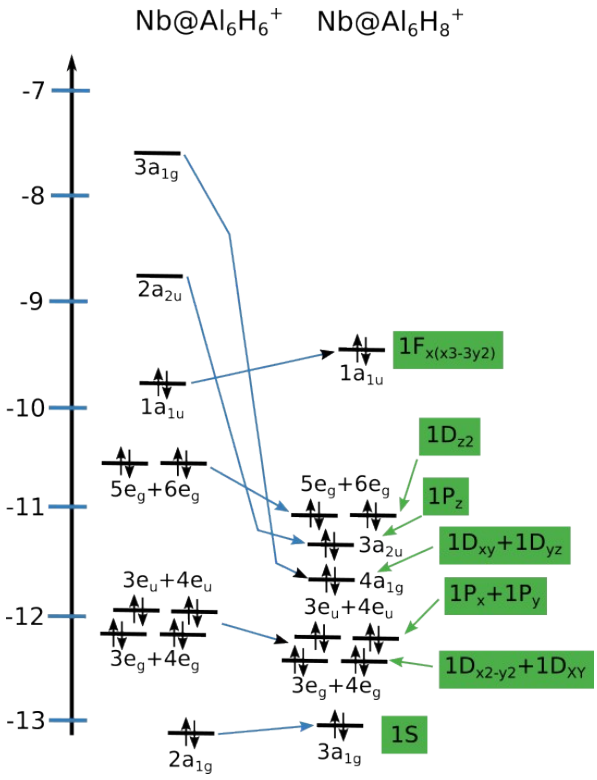

Figure S9. Comparison of the orbital energy diagrams of $Nb@Al_6H_6^+$ and $Nb@Al_8H_8^+$. The blue arrows highlight the correlation between both.

7) Density of states analysis of $NbAl_8H_8^+$ (Iso2)

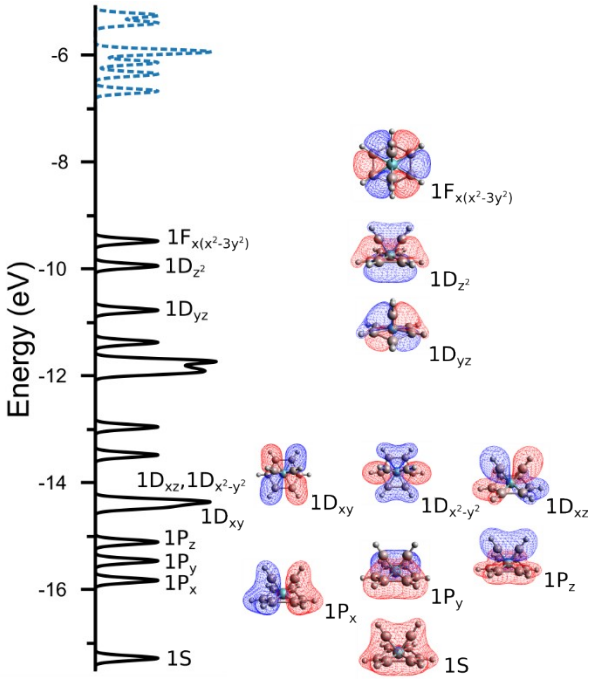

Figure S10. Density of states of the $NbAl_8H_8^+$ (Iso2) cluster. Occupied (empty) states are represented by a full black (dashed blue) line. Molecular orbitals of delocalized character are shown on the right side of the figure, with a label of their corresponding symmetry (TPSSh/aug-cc-pVTZ-PP).

8) Intensity of $NbAl_n^+$ clusters after photofragmentation

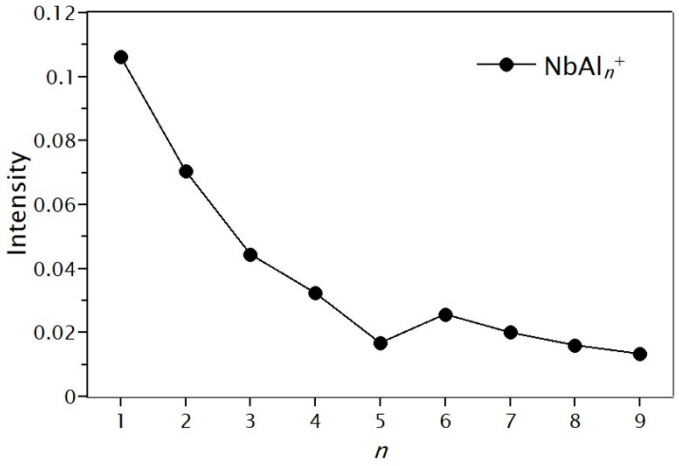

Figure S11. Integrated intensity in a mass spectrum of metallic $NbAl_n^+$ clusters. The spectrum is recorded after the clusters are exposed to the laser light of a focused F_2 laser (157 nm), which induces intensive fragmentation prior detection in the mass spectrometer. Under these conditions, the intensities carry information about the relative stabilities of the clusters (see *Phys. Rev. A* 2018, **97**, 052508 for details), with higher values for more stable clusters. As seen, the metallic $NbAl_8^+$ is not a particular size in this series.